

# Omnidirectional Vision-Based Formation Control\*

René Vidal      Omid Shakernia      Shankar Sastry

Department of Electrical Engineering and Computer Sciences  
University of California at Berkeley, Berkeley CA 94720-1774  
{rvidal,omids,sastry}@eecs.berkeley.edu

## Abstract

We consider the problem of distributed leader-follower formation control for nonholonomic mobile robots equipped with paracatadioptric cameras. Our approach is to translate the formation control problem from the configuration space into a separate visual servoing task for each follower. First, we present an algorithm for infinitesimal multi-body motion segmentation from multiple paracatadioptric views. We derive a rank constraint on the optical flows across many frames, from which one can estimate the position of each leader in the paracatadioptric image plane of the follower. Then, we study the relative leader-follower kinematics in the catadioptric image plane and design a tracking controller for each follower using feedback linearization techniques. Finally, we present experimental results on multi-body motion segmentation of a real image sequence and simulation results on vision-based formation control.

## 1 Introduction

Formation control of unmanned ground and aerial vehicles is gaining significant importance in the control and robotics communities thanks to recent advances in communication and computer vision. Examples of formation control are ubiquitous in nature and in man-made devices, from bird flight and fish swimming to air traffic control, satellite clustering, automatic highways, and mobile robotics.

Previous work in formation control assumed that communication among the robots is available and concentrated on the study of the stability and feasibility of formations. Swaroop et.al [23] proposed the notion of string stability for line formations. They showed that, although the pair-wise leader-follower system can be stable, the overall formation can become unstable due to propagation of errors through the string. The authors showed that a string formation is stabilizable when each follower has access to the leader's state. Pant et.al [16] generalized this notion to formations in a planar mesh, through the concept of mesh stability. Tannner [25] concentrated on formations in acyclic graphs and showed that the structure of the interconnections and the amount of information can affect the input-to-state stability of the formation. Fax et.al [8] analyzed the stability of formations in arbitrary graphs and proposed a Nyquist-like stability criteria that can be derived from the spectral properties of the graph Laplacians. Tabuada et.al [24] studied the conditions under which a desired formation is feasible, *i.e.* whether it is possible

---

\*This research is supported by ONR grant N00014-00-1-0621.

to design a trajectory that both maintains the formation and satisfies the kinematic constraints of the agents. They showed that in order for a formation to be feasible, certain differential-geometric conditions need to be satisfied.

In the *absence of communication*, the formation control problem becomes quite challenging from a sensing viewpoint, since one is faced with the problem of simultaneously estimating the motion of multiple moving objects. Previous work [7] avoids this difficulty by painting each leader of a different color and then using color tracking to identify them. Here we consider the case in which the detection of the leaders is based solely on their motion information on the image plane.

At present (see [13]), there are many *perspective* and *orthographic* structure from motion algorithms for analyzing a *static* scene, i.e. a scene in which the camera is moving and the world is static or viceversa. The study of *dynamic* scenes, i.e. scenes in which both the camera and multiple objects move independently, is much more recent and only partially understood. The main difficulty relies on the need of simultaneous motion estimation (rotation and translation of the target relative to the camera) and motion segmentation (determination of the pixels in the image that belong to each moving target). Previous work includes the case of points moving linearly with constant speed [12, 20] or in a conic section [1], multiple moving objects seen by an orthographic camera [5, 14], or motion segmentation from two perspective views [27]. For central panoramic cameras [2], there exist two-view motion estimation algorithms both in the discrete [22, 10, 4] and in the differential case [11, 26]. More recently, multi-frame algorithms were proposed both in the discrete [21] and in the differential case [18]. To the best of our knowledge, there is no work on the analysis of dynamic scenes seen by a central panoramic camera.

## 1.1 Contributions of this work

We consider the problem of distributed leader-follower formation control for nonholonomic mobile robots equipped with paracatadioptric cameras. Our work differs from previous work on vision-based formation control for mobile robots, such as [6], in that our control laws are defined in the paracatadioptric image plane. Our approach is to translate the formation control problem from the configuration space into a separate visual servoing control task for each follower. In Section 2, we develop an algorithm for infinitesimal multi-body motion segmentation from multiple paracatadioptric views. We derive a rank constraint on the paracatadioptric optical flows across many frames, from which one can estimate the position of each leader in the image plane of the follower. In Section 3 we derive the leader-follower dynamical equations in the paracatadioptric image plane using a nonholonomic kinematic model for the motion of the robots and use feedback linearization techniques to design a tracking controller for each follower. In Section 4 we present experimental results on multi-body motion segmentation of a real image sequence. We also present simulation results validating our vision-based formation control scheme.

## 2 Paracatadioptric Motion Segmentation

### 2.1 Paracatadioptric projection model

A paracatadioptric camera [9] projects a 3D point  $q = (X, Y, Z)^T$  onto the image plane by first projecting  $q$  onto the surface  $Z = \frac{1}{2}(X^2 + Y^2 - 1)$  which represents a paraboloidal mirror of focal length  $1/2$  with focus at the origin; and then orthographically projecting the back-projection ray  $\mathbf{b}$  onto the plane  $Z = 0$  (see Figure 1). The composition of these two projections gives:

$$\begin{bmatrix} x \\ y \end{bmatrix} = \frac{1}{-Z + \sqrt{X^2 + Y^2 + Z^2}} \begin{bmatrix} X \\ Y \end{bmatrix} \triangleq \frac{1}{\lambda} \begin{bmatrix} X \\ Y \end{bmatrix}. \quad (1)$$

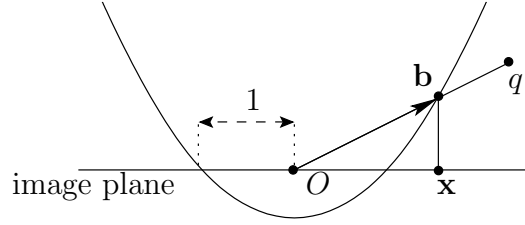


Figure 1: Showing the projection model for paracatadioptric cameras, and the back-projection ray  $\mathbf{b}$  associated with image point  $\mathbf{x}$ .

### 2.2 Paracatadioptric optical flow

If the camera undergoes a linear velocity  $V \in \mathbb{R}^3$  and an angular velocity  $\Omega \in \mathbb{R}^3$ , then the coordinates of  $q$  in the camera frame evolve as  $\dot{q} = \Omega \times q + V$ . The motion of the camera induces a motion in the paracatadioptric image plane, which can be computed by differentiating (1) with respect to time. We showed in [18] that the optical flow  $(\dot{x}, \dot{y})^T$  induced by a paracatadioptric camera undergoing a motion  $(\Omega, V)$  is given by:

$$\begin{bmatrix} \dot{x} \\ \dot{y} \end{bmatrix} = \begin{bmatrix} xy & z-x^2 & -y \\ y^2-z & -xy & x \end{bmatrix} \Omega + \frac{1}{\lambda} \begin{bmatrix} \frac{1+z-x^2}{1+z} & \frac{-xy}{1+z} & \frac{x}{1+z} \\ \frac{-xy}{1+z} & \frac{1+z-y^2}{1+z} & \frac{y}{1+z} \end{bmatrix} V.$$

where  $z \triangleq (x^2 + y^2 - 1)/2$  and  $\lambda \triangleq -Z + \sqrt{X^2 + Y^2 + Z^2}$ .

If the camera is attached to a mobile robot moving on the ground plane with the optical axis parallel to the  $Z$  axis, then the angular velocity is  $\Omega = (0, 0, \Omega_z)^T$  and the linear velocity is  $V = (V_x, V_y, 0)^T$ . Thus the optical flow equation can be simplified as:

$$\begin{bmatrix} \dot{x} \\ \dot{y} \end{bmatrix} = \begin{bmatrix} -y \\ x \end{bmatrix} \Omega_z + \frac{1}{\lambda} \begin{bmatrix} \frac{1+z-x^2}{1+z} & \frac{-xy}{1+z} \\ \frac{-xy}{1+z} & \frac{1+z-y^2}{1+z} \end{bmatrix} \begin{bmatrix} V_x \\ V_y \end{bmatrix}. \quad (2)$$

### 2.3 Paracatadioptric Motion Segmentation

Let  $(x_i, y_i)$ ,  $i = 1, \dots, n$ , be a pixel in the zero-th frame, and imagine we are given measurements of its optical flow  $(\dot{x}_{ij}, \dot{y}_{ij})$  in frame  $j = 1, \dots, m$  relative to the zero-th. If the scene is static, then from (2) we get

$$\begin{bmatrix} \dot{x}_{ij} & \dot{y}_{ij} \end{bmatrix} = S_i M_j^T$$

where

$$S_i = \begin{bmatrix} x_i & -y_i & \frac{1+z_i-x_i^2}{(1+z_i)\lambda_i} & \frac{-x_i y_i}{(1+z_i)\lambda_i} & \frac{1+z_i-y_i^2}{(1+z_i)\lambda_i} \end{bmatrix} \in \mathbb{R}^{1 \times 5}, \quad M_j = \begin{bmatrix} 0 & \Omega_{zj} & V_{xj} & V_{yj} & 0 \\ \Omega_{zj} & 0 & 0 & V_{xj} & V_{yj} \end{bmatrix} \in \mathbb{R}^{2 \times 5}.$$

Therefore the *optical flow matrix*  $W \in \mathbb{R}^{n \times 2m}$  satisfies

$$W \triangleq \begin{bmatrix} \dot{x}_{11} & \dot{y}_{11} & \cdots & \cdots & \dot{x}_{1m} & \dot{y}_{1m} \\ \vdots & \vdots & & & \vdots & \vdots \\ \dot{x}_{n1} & \dot{y}_{n1} & \cdots & \cdots & \dot{x}_{nm} & \dot{y}_{nm} \end{bmatrix} = SM^T, \quad (3)$$

where  $S = [S_1^T \ S_2^T \ \cdots \ S_n^T]^T \in \mathbb{R}^{n \times 5}$  is the structure matrix and  $M = [M_1^T \ M_2^T \ \cdots \ M_m^T]^T \in \mathbb{R}^{2m \times 5}$  is the motion matrix. We conclude that, for a static scene taken from a paracatadioptric camera moving on a plane, the collection of optical flows across many frames lies on a 5-dimensional subspace of  $\mathbb{R}^{2m}$ .

For a dynamic scene with  $k$  independent motions, the optical flow matrix can be decomposed as

$$W = \begin{bmatrix} S_1 & \cdots & 0 \\ \vdots & \ddots & \vdots \\ 0 & \cdots & S_k \end{bmatrix} \begin{bmatrix} M_1^T \\ \vdots \\ M_k^T \end{bmatrix} = SM^T \quad (4)$$

where  $S \in \mathbb{R}^{n \times 5k}$  and  $M \in \mathbb{R}^{2m \times 5k}$ . We showed in [19] that the block diagonal structure of  $W$  implies that its leading singular vector will have the same value for pixels corresponding to the same motion. Furthermore, the eigenvector has a different value for pixels corresponding to different motions. This gives an effective criterion for segmenting the pixels of the current frame into a collection of  $k$  groups corresponding to the independent motions. One of these groups corresponds to the motion of the camera, which is generated by the static background. For a formation control scenario, this group can always be identified as the largest one.

### 3 Omnidirectional Vision-Based Formation Control

In the previous section, we presented the equations of motion of a pixel in the paracatadioptric image plane and proposed an algorithm for segmenting the image into  $k$  groups corresponding to independent motions. In doing so, we assumed that the camera and the observed objects undergo arbitrary motions. In this section, we derive the equations of motion in the particular case of a leader-follower configuration in the  $XY$  plane, with the paracatadioptric camera mounted on-board the follower. We assume that the mounting is such that the coordinate system of the on-board camera coincides with the robot coordinate system, thus the camera's optical center is located at  $(X, Y, Z) = 0$  in the follower frame. We then derive a tracking controller for each follower to maintain the desired formation.

#### 3.1 Relative leader-follower kinematics

Let us start with the simplest case of a single follower tracking a leader. Let  $(R_f(t), T_f(t)) \in SE(3)$  and  $(R_\ell(t), T_\ell(t)) \in SE(3)$  be the poses of the follower and that of the leader at time  $t$  with respect to a fixed reference frame. Let  $q \in \mathbb{R}^3$  be a point located on the

leader but written in the follower frame. The coordinates of  $q$  relative to the reference frame are  $q_\ell(t) = R_\ell(t)q + T_\ell(t)$  and the coordinates of  $q$  relative to the follower frame are:

$$q_{\ell f}(t) = R_f^T(t)R_\ell(t)q + R_f^T(t)(T_\ell(t) - T_f(t)). \quad (5)$$

Differentiating (5) yields:

$$\dot{q}_{\ell f} = (\dot{R}_f^T R_\ell + R_f^T \dot{R}_\ell)q + \dot{R}_f^T(T_\ell - T_f) + R_f^T(\dot{T}_\ell - \dot{T}_f). \quad (6)$$

Combining (5) and (6) gives:

$$\dot{q}_{\ell f} = (\dot{R}_f^T R_f + R_f^T \dot{R}_\ell R_\ell^T R_f)q_{\ell f} + R_p^T(\dot{T}_e - \dot{T}_p - \dot{R}_e R_e^T(T_e - T_p)). \quad (7)$$

Let  $\widehat{\Omega} \in so(3)$  be the skew-symmetric matrix generating the cross product, i.e.  $\widehat{\Omega}q = \Omega \times q$  for all  $q \in \mathbb{R}^3$ . Since  $\dot{R}R^T \in so(3)$ ,  $\widehat{R^T \widehat{\Omega} R} = R^T \widehat{\Omega} R$  and  $\dot{R}^T R = -R^T \dot{R} R^T$  [15], we may define the angular velocities  $\Omega_f, \Omega_\ell \in \mathbb{R}^3$  by:

$$\widehat{\Omega}_\ell = \dot{R}_\ell R_\ell^T \quad \text{and} \quad \widehat{\Omega}_f = \dot{R}_f R_f^T. \quad (8)$$

Combining (7) and (8) yields:

$$\dot{q}_{\ell f} = [R_f^T(\Omega_\ell - \Omega_f)] \times q_{\ell f} + R_f^T(\dot{T}_\ell - \dot{T}_f - \widehat{\Omega}_\ell(T_\ell - T_f)) \triangleq \widehat{\Omega}_{\ell f} q_{\ell f} + V_{\ell f}, \quad (9)$$

where  $\Omega_{\ell f}$  and  $V_{\ell f}$ , defined by the equation above, are the angular and translational velocities of the leader relative to the follower.

## 3.2 Nonholonomic mobile robot dynamics

We consider a nonholonomic kinematic model for the dynamics of the ground robots. The dynamics of the  $i$ -th robot are given by:

$$\dot{X}_i = v_i \cos \theta_i, \quad \dot{Y}_i = v_i \sin \theta_i, \quad \dot{\theta}_i = \omega_i \quad (10)$$

where the state  $(X_i, Y_i, \theta_i) \in SE(2)$ , and the inputs  $v_i$  and  $\omega_i$  are the linear and angular velocities, respectively. Letting  $T_i = (X_i, Y_i, 0)^T \in \mathbb{R}^3$ ,  $e_3 = (0, 0, 1)^T \in \mathbb{R}^3$ ,  $R_i = \exp(\widehat{e}_3 \theta_i) \in SO(3)$ ,  $\Omega_i = (0, 0, \omega_i)^T \in \mathbb{R}^3$  and replacing in (9) we obtain:

$$\Omega_{\ell f} = \begin{bmatrix} 0 \\ 0 \\ 1 \end{bmatrix} (\omega_\ell - \omega_f), \quad V_{\ell f} = - \begin{bmatrix} 1 \\ 0 \\ 0 \end{bmatrix} v_f + \begin{bmatrix} F_{\ell f} \\ 0 \end{bmatrix} \quad (11)$$

where  $F_{\ell f} \triangleq F_{\ell f}(T_\ell, T_f, \theta_\ell, \theta_f, v_\ell, \omega_\ell) \in \mathbb{R}^2$  is given by:

$$\begin{bmatrix} \cos(\theta_\ell - \theta_f) \\ \sin(\theta_\ell - \theta_f) \end{bmatrix} v_\ell - \begin{bmatrix} \cos(\theta_f) & \sin(\theta_f) \\ -\sin(\theta_f) & \cos(\theta_f) \end{bmatrix} \begin{bmatrix} -(Y_\ell - Y_f) \\ X_\ell - X_f \end{bmatrix} \omega_\ell.$$

### 3.3 Paracatadioptric leader-follower dynamics

Replacing the expressions for  $\Omega_{\ell f}$  and  $V_{\ell f}$  in (2), we obtain the following equations for the motion of a pixel in the paracatadioptric plane:

$$\begin{bmatrix} \dot{x} \\ \dot{y} \end{bmatrix} = - \begin{bmatrix} \frac{1+z-x^2}{(1+z)\lambda} & -y \\ \frac{-xy}{(1+z)\lambda} & x \end{bmatrix} \begin{bmatrix} v_f \\ \omega_f \end{bmatrix} + \begin{bmatrix} \frac{1+z-x^2}{(1+z)\lambda} & \frac{-xy}{(1+z)\lambda} & -y \\ \frac{-xy}{(1+z)\lambda} & \frac{1+z-y^2}{(1+z)\lambda} & x \end{bmatrix} \begin{bmatrix} F_{\ell f} \\ \omega_\ell \end{bmatrix}.$$

Since  $z = (x^2 + y^2 - 1)/2$  and  $\lambda = 2Z/(x^2 + y^2 - 1) = Z/z$ , if we assume a ground plane constraint, i.e. if we assume that  $Z = Z_{\text{ground}} < 0$  is known, then we can write the equations of motion of a pixel as the drift-free control system:

$$\begin{bmatrix} \dot{x} \\ \dot{y} \end{bmatrix} = H(x, y)\mathbf{u}_f + G(x, y)\mathbf{d}_{\ell f} \quad (12)$$

where  $\mathbf{u}_f = (v_f, \omega_f) \in \mathbb{R}^2$  is the control action for the follower and  $\mathbf{d}_{\ell f} = (F_{\ell f}, \omega_\ell) \in \mathbb{R}^3$  can be thought of as an external input that depends on the state and control action of the leader and the state of the follower.

### 3.4 Omnidirectional visual servoing

We now design a control law for the follower to keep a desired distance  $r_d$  and an angle  $\alpha_d$  from the leader. Although the desired formation is usually specified in the configuration space, under the ground plane assumption such a formation can always be converted into a desired formation in image space. Hence we assume that we are given a desired pixel location  $(x_d, y_d)$  for the leader in the image plane of the follower, where  $(x_d, y_d) = (r_d \cos(\alpha_d), r_d \sin(\alpha_d))$ .

We now apply feedback linearization to the control system (12) with output  $(x, y)$ . We observe that the system has a well defined vector relative degree<sup>1</sup> of  $(1, 1)$  for all pixels  $(x, y)$  such that  $H(x, y)$  is of rank 2, i.e. whenever  $x \neq 0$  and  $x^2 + y^2 \neq 1$ . We assume that  $x \neq 0$  and  $x^2 + y^2 \neq 1$  from now on<sup>2</sup>. In this case, the relative degree of the system is  $1 + 1 = 2$  thus the zero dynamics of the system are trivially exponentially minimum phase. Therefore the control law

$$\mathbf{u}_f = -H(x, y)^{-1} \left( G(x, y)\mathbf{d}_{\ell f} + \begin{bmatrix} k_1(x - x_d) \\ k_2(y - y_d) \end{bmatrix} \right) \quad (13)$$

results in a locally exponentially stable system around  $(x_d, y_d)$  whenever  $k_1 > 0$  and  $k_2 > 0$ .

In order to achieve exact inversion and tracking using the control law (13), it is necessary to measure the effect of the unknown external input  $G_{\ell f}\mathbf{d}_{\ell f} \in \mathbb{R}^2$ . Although this term is a function of the state and control of the leader and the state of the follower, we emphasize here that it is *not* necessary to measure any of these quantities. Instead, we only need to estimate the two-dimensional vector  $G_{\ell f}\mathbf{d}_{\ell f}$ . Furthermore, such a vector can be easily estimated using the image measurements provided by the motion segmentation techniques developed in Section 2.3 as we show below.

<sup>1</sup>See [17] page 408 for the definition of relative degree.

<sup>2</sup>The degenerate configuration  $x = 0$  is due to the nonholonomy of the follower's dynamics, while the degenerate configuration  $x^2 + y^2 = 1$  corresponds to the projection of the horizon, hence it is due to the paracatadioptric camera model.

Let  $(x_w, y_w)$  and  $(\dot{x}_w, \dot{y}_w)$  be the position and optical flow of a pixel that corresponds to a static 3D point in the world. From (12), the velocities of the follower causing that optical flow are given by<sup>3</sup>:

$$\mathbf{u}_f = H(x_w, y_w)^{-1} \begin{bmatrix} \dot{x}_w \\ \dot{y}_w \end{bmatrix}. \quad (14)$$

Notice that in the presence of noise one may improve the estimation of  $\mathbf{u}_f$  in (14) by using more than one pixel and solving the equations in a least squares sense.

Now let  $(x_\ell, y_\ell)$  and  $(\dot{x}_\ell, \dot{y}_\ell)$  be the position and optical flow of a pixel that corresponds to a 3D point on the leader. From (12) we have:

$$G(x_\ell, y_\ell)\mathbf{d}_{\ell f} = \begin{bmatrix} \dot{x}_\ell \\ \dot{y}_\ell \end{bmatrix} - H(x_\ell, y_\ell)H(x_w, y_w)^{-1} \begin{bmatrix} \dot{x}_w \\ \dot{y}_w \end{bmatrix}. \quad (15)$$

## 4 Experimental Results

We tested the proposed motion segmentation algorithm in a real image sequence. Figure 2(a) shows one out of 200 frames taken by a paracatadioptric camera observing two moving robots. The optical flow was computed using Black's algorithm [3]. Figure 2(b) shows the results of applying the segmentation algorithm described in Section 2.3. The image sequence is correctly segmented into two independent motions.

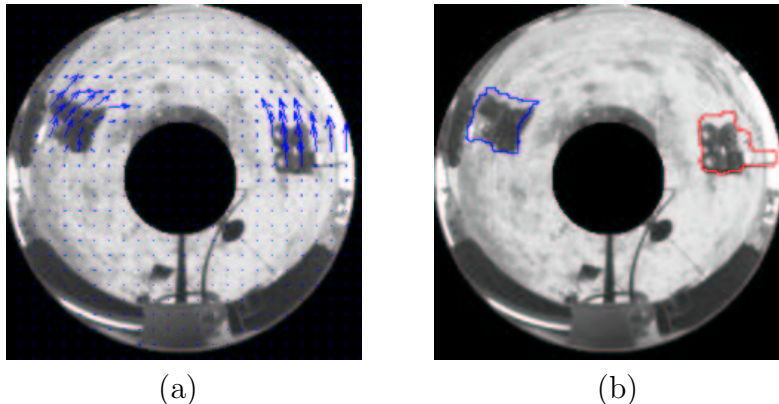


Figure 2: An example of motion segmentation based on paracatadioptric optical flow. (a) One frame of the sequence with optical flow superimposed. (b) Segmentation results.

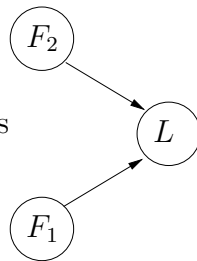


Figure 3: A V-Formation configuration.

---

<sup>3</sup>Notice that since the point in 3D space is static, i.e.  $(v_l, \omega_l) = (0, 0)$ , the second term in (12) is zero.

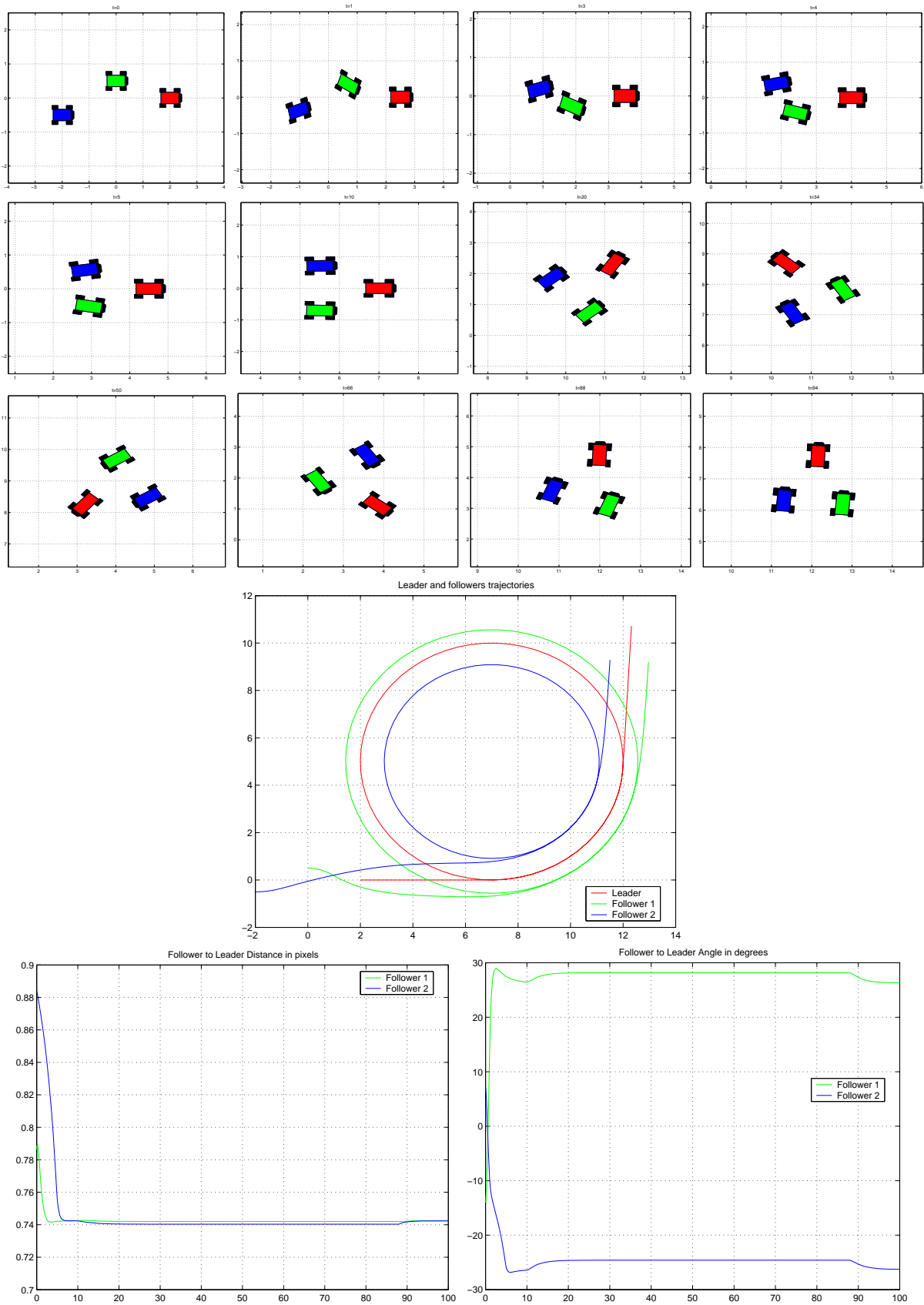


Figure 4: Simulation results for a V-Formation. For  $t \in [0, 10]$  the followers flip positions from the initial configuration to the desired one. For  $t > 10$  the followers maintain their formation into a full circle and then into a line.

We also tested the proposed formation control algorithm on the V-Formation configuration shown in Figure 3. The control parameters were chosen as  $k_1 = 2.5$ ,  $k_2 = 1.76$ . Figure 4 shows simulation results for a desired configuration  $(r_d, \alpha_d) = (1/\sqrt{2}, \pi/6)$  for Follower1 (green) and  $(r_d, \alpha_d) = (1/\sqrt{2}, -\pi/6)$  for Follower2 (blue). For  $t \in [0, 10]$ , the followers move from the initial configuration to the desired one by flipping sides with respect to the leader, which moves at constant velocities  $v_\ell = 0.5$  and  $w_\ell = 0$ . For  $t \in [10, 88]$ , the leader changes its angular velocity to  $w_\ell = 0.1$ , thus starting a circular motion. The followers maintain the formation by moving on circles of different radii depending on the side of the leader on which they are located. For  $t \in [10, 88]$  the leader changes its angular velocity back to  $w_\ell = 0$ , thus moving in a straight line. The followers maintain the formation by moving in a straight line as well. It is important to mention that, while the followers maintain formation with the leader, they cannot achieve zero error. This is due to the nonholonomic nature of the robots. Consider for example a leader-follower configuration with the leader moving in a circle. Then the follower cannot follow the leader at a desired distance with a desired angle of zero degrees, because the tangents to the circle at two different points are not the same.

## 5 Conclusions

We have presented a framework for distributed formation control of nonholonomic mobile robots equipped with paracatadioptric cameras. We presented an algorithm for infinitesimal multi-body motion segmentation from multiple paracatadioptric views that provides an estimate of the current position of each leader in the image plane of the follower. We solved the formation control problem by designing a distributed control law that follows a desired formation specified in the paracatadioptric image plane. We presented experimental results for motion segmentation and simulation results for formation control.

## References

- [1] S. Avidan and A. Shashua. Trajectory triangulation: 3D reconstruction of moving points from a monocular image sequence. *IEEE Trans. on Pattern Analysis and Machine Intelligence*, 22(4):348–357, 2000.
- [2] S. Baker and S. Nayar. A theory of single-viewpoint catadioptric image formation. *International Journal on Computer Vision*, 35:175–196, 1999.
- [3] M. Black. <http://www.cs.brown.edu/people/black/ignc.html>, 1996.
- [4] P. Chang and M. Hebert. Omni-directional structure from motion. In *IEEE Workshop on Omnidirectional Vision*, pages 127–133, June 2000.
- [5] J. Costeira and T. Kanade. Multi-body factorization methods for motion analysis. In *IEEE International Conference on Computer Vision*, pages 1071–1076, 1995.
- [6] A. Das, R. Fierro, V. Kumar, J. Ostrowski, J. Spletzer, and C. Taylor. A framework for vision based formation control. *Multi-Robot Systems: A Special Issue of IEEE Transactions on Robotics and Automation*, 2002. Submitted.
- [7] A. Das, R. Fierro, V. Kumar, B. Southall, J. Spletzer, and C.J. Taylor. Real-time vision-based control of a nonholonomic mobile robot. In *IEEE Conference on Robotics and Automation*, pages 1714–1719, Seoul, Korea, May 2001.
- [8] A. Fax and R. Murray. Graph laplacians and stabilization of vehicle formations. In *International Federation of Automatic Control World Congress*, 2002.

- [9] C. Geyer and K. Daniilidis. A unifying theory for central panoramic systems and practical implications. In *Proceedings of the European Conference on Computer Vision*, 2000.
- [10] C. Geyer and K. Daniilidis. Structure and motion from uncalibrated catadioptric views. In *IEEE Conference on Computer Vision and Pattern Recognition.*, pages 279–286, 2001.
- [11] J. Gluckman and S.K. Nayar. Ego-motion and omnidirectional cameras. In *Proceedings of IEEE 6th International Conference on Computer Vision*, pages 999–1005, 1998.
- [12] M. Han and T. Kanade. Reconstruction of a scene with multiple linearly moving objects. In *Int. Conference on Computer Vision and Pattern Recognition*, vol. 2, pp. 542–549, 2000.
- [13] R. Hartley and A. Zisserman. *Multiple View Geometry in Computer Vision*. Cambridge, 2000.
- [14] K. Kanatani. Motion segmentation by subspace separation and model selection. In *IEEE International Conference on Computer Vision*, volume 2, pages 586–591, 2001.
- [15] R. M. Murray, Z. Li, and S. S. Sastry. *A Mathematical Introduction to Robotic Manipulation*. CRC press Inc., 1994.
- [16] A. Pant, P. Seiler, T. Koo, and K. Hedrick. Mesh stability of unmanned aerial vehicle clusters. In *American Control Conference*, pages 62–68, 2001.
- [17] S. Sastry. *Nonlinear Systems: Analysis, Stability and Control*. Springer, 1999.
- [18] O. Shakernia, R. Vidal, and S. Sastry. Infinitesimal motion estimation from multiple central panoramic views. In *Workshop on Motion and Video Computing*, 2002. (To appear).
- [19] O. Shakernia, R. Vidal, and S. Sastry. Multi-body motion estimation and segmentation from multiple central panoramic views. In *IEEE Int. Conf. on Robotics and Automation*, 2003. Submitted.
- [20] A. Shashua and A. Levin. Multi-frame infinitesimal motion model for the reconstruction of (dynamic) scenes with multiple linearly moving objects. In *IEEE International Conference on Computer Vision*, volume 2, pages 592–599, 2001.
- [21] P. Sturm. Mixing catadioptric and perspective cameras. In *ECCV Workshop on Omnidirectional Vision*, pages 37–44, 2002.
- [22] T. Svoboda, T. Pajdla, and V. Hlavac. Epipolar geometry for panoramic cameras. In *5th European Conference on Computer Vision*, pages 218–231, 1998.
- [23] D. Swaroop and J. Hedrick. String stability of interconnected systems. *IEEE Transactions on Automatic Control*, 41:349–357, 1996.
- [24] P. Tabuada, G. Pappas, and P. Lima. Feasible formations of multi-agent systems. In *American Control Conference*, pages 56–61, 2001.
- [25] H. Tanner, V. Kumar, and G. Pappas. The effect of feedback and feedforward on formation ISS. In *IEEE Int. Conference on Robotics and Automation*, pages 3448–3453, 2002.
- [26] R.F. Vassallo, J. Santos-Victor, and J. Schneebeli. A general approach for egomotion estimation with omnidirectional images. In *Proceedings of IEEE Workshop on Omnidirectional Vision*, pages 97–103, 2002.
- [27] R. Vidal, S. Soatto, Y. Ma, and S. Sastry. Segmentation of dynamic scenes from the multibody fundamental matrix. *Workshop on Visual Modeling of Dynamic Scenes*, 2002.